Inter-strand C—H···O hydrogen bonds stabilizing four-stranded intercalated molecules: Stereoelectronic effects of O4' in cytosine-rich DNA

(base-ribose stacking/sugar pucker/x-ray crystallography)

IMRE BERGER[†], MARTIN EGLI[‡], AND ALEXANDER RICH[†]

[†]Department of Biology, Massachusetts Institute of Technology, Cambridge, MA 02139; and [‡]Department of Molecular Pharmacology and Biological Chemistry, Northwestern University Medical School, 303 East Chicago Avenue, Chicago, IL 60611-3008

ABSTRACT DNA fragments with stretches of cytosine residues can fold into four-stranded structures in which two parallel duplexes, held together by hemiprotonated cytosine·cytosine$^+$ (C·C$^+$) base pairs, intercalate into each other with opposite polarity. The structural details of this intercalated DNA quadruplex have been assessed by solution NMR and single crystal x-ray diffraction studies of cytosine-rich sequences, including those present in metazoan telomeres. A conserved feature of these structures is the absence of stabilizing stacking interactions between the aromatic ring systems of adjacent C·C$^+$ base pairs from intercalated duplexes. Effective stacking involves only the exocyclic keto groups and amino groups of the cytidine bases. The apparent absence of stability provided by stacking interactions between the bases in this intercalated DNA has prompted us to examine the available structures in detail, in particular with regard to unusual features that could compensate for the lack of base stacking. In addition to base-on-deoxyribose stacking and intra-cytidine C—H···O hydrogen bonds, this analysis reveals the presence of a hitherto unobserved, systematic intermolecular C—H···O hydrogen bonding network between the deoxyribose sugar moieties of antiparallel backbones in the four-stranded molecule.

The DNA intercalation motif, a four-stranded arrangement of two parallel intercalating duplexes using C·C$^+$ base pairs, is adopted by a variety of cytosine-rich DNA fragments. Detailed NMR or x-ray diffraction studies were conducted thus far for d(TC$_5$) (1), d(C$_4$) (2), d(CCCT) (3), d(TCC) and d(5^{Me}CCT) (4), d(CCCAAT) (5), and d(TAACCC) (6). In the four crystal structures (2, 3, 5, 6) the intercalated cytosine segments show a globally similar arrangement, with the remaining nucleotides folded into a variety of motifs, including A·A·T base triplets (5) and trinucleotide loops (6). Important geometrical features displayed by the two parallel-stranded duplexes forming the intercalation motif are a slow right-handed helical twist (12–20°), a rise of approximately 6.2 Å between covalently linked residues, and planar base pairing between cytosines around a 2-fold rotation axis requiring hemiprotonation at the N3 position. The two duplexes are intercalated with opposite polarity and form a quasi two-dimensional array. The structure has two broad and two narrow grooves with the antiparallel backbone pairs from intercalated duplexes in van der Waals contact in the narrow grooves. Thus, the intercalation motif is dramatically different in its architecture compared with A-, B-, or Z-form duplex DNA and also the guanine quadruplex (7, 8). It is characterized by two features, both of which one is inclined to attribute as destabilizing influences. First, there is the almost complete absence of overlap between adjacent aromatic cytosine ring systems from intercalated duplexes (Fig. 1A). Second, unusually close intermolecular contacts between sugar-phosphate backbones in the narrow grooves are observed, with inter-strand phosphorus–phosphorus distances as close as 5.9 Å (5), presumably resulting in unfavorable electrostatic repulsion if not shielded by cations or bridging water molecules.

The close contacts between pairs of antiparallel sugar-phosphate backbones from the two interdigitated duplexes are a unique characteristic of four-stranded intercalated DNA. Indeed, the unusually strong nuclear overhauser effect signals between inter-strand sugar H1' protons and H1' and H4' protons constitute a fingerprint of this molecule, as such close backbone–backbone interactions do not exist in any of the other two-, three-, or four-stranded DNA structures (1, 2, 9). Here we show that these close contacts between hydrogen atoms from adjacent sugar moieties in the two strands are the consequence of stabilizing C—H···O type hydrogen bonds between neighboring deoxyriboses. Accordingly, the O4' oxygen atom of a deoxyribose from one strand is found to form a hydrogen bond to C1'–H1' of a deoxyribose from the neighboring strand in the narrow groove, and vice versa. However, close inspection of the relative orientations of such deoxyribose pairs reveals that these interactions are not completely symmetrical. Thus, a lone electron pair of one O4' is directed toward the H1' hydrogen from the neighboring sugar, whereas the corresponding lone electron pair of the O4' from the latter appears to be shared among the neighboring H1' and H4' hydrogens. Consequently, a systematic C—H···O bonding network is formed between the antiparallel strands in the narrow grooves of four-stranded intercalated DNA. In addition, at some intercalation steps the intercalation motif is stabilized by intra-cytidine C—H···O hydrogen bonds, previously observed in left-handed Z-DNA (10). The crystal structure of d(CCCAAT) additionally displays stabilizing base-on-deoxyribose stacking between adjacent cytosine and adenine residues. Such stacking interactions appear to be a recurring feature in nucleic acid structures and were shown to provide stability in Z-DNA, in complexes between DNA and minor groove binding drugs, as well as in large RNA molecules (ref. 10 and references therein].

It is now widely accepted that short C—H···O contacts constitute electrostatically stabilized attractive interactions, which can be considered hydrogen bonds (11–13). A survey of 113 accurate neutron diffraction crystal structures clearly indicated their widespread occurrence (11). They were observed in the crystal structures of nucleosides and nucleotides (14) and may contribute to the stability of nucleic acid base pairs (15). C—H···O hydrogen bonds between water molecules and purines, pyrimidines, amino acids, alkaloids, and others were found in the crystal structures of hydrates of these molecules (16) and are thought to stabilize the conformations of the anticodon loop in tRNA (17) and β-sheets in proteins (18). The energy of the C—H···O interaction was calculated to
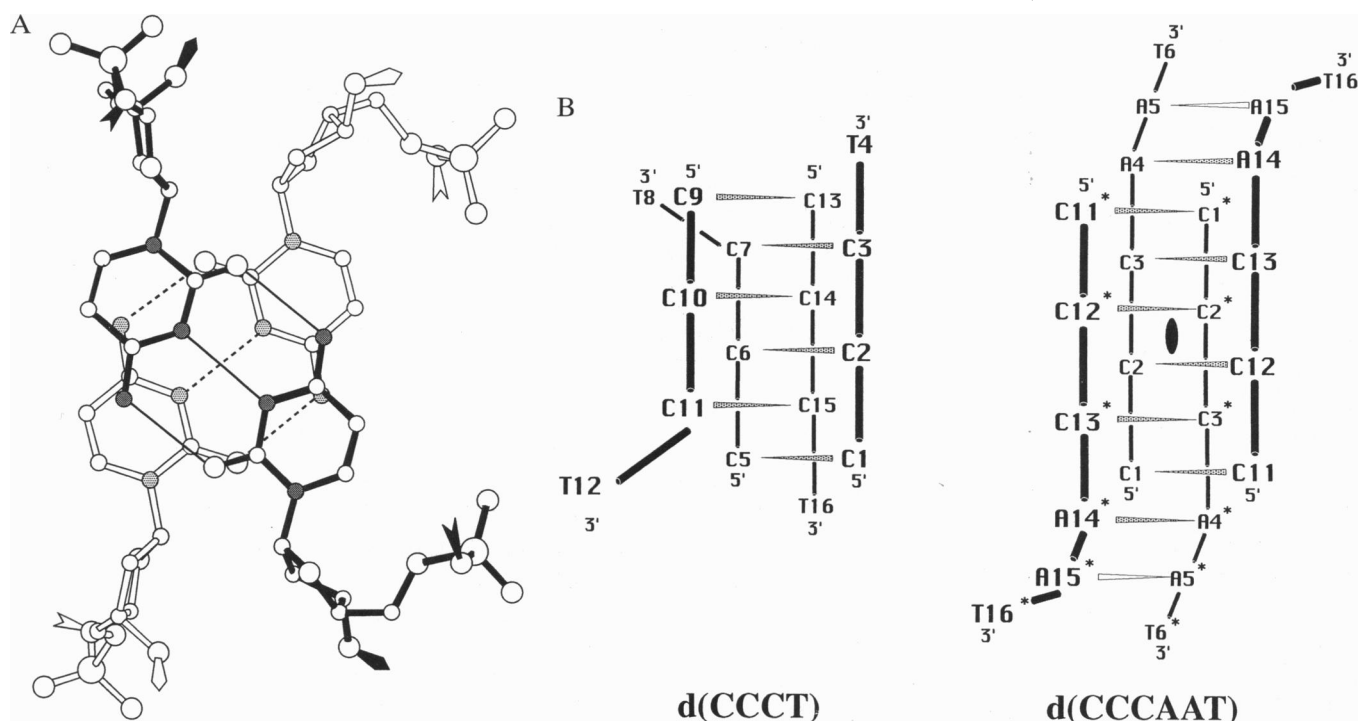
FIG. 1. Architecture of the intercalation motif. (*A*) Characteristic stacking pattern between adjacent cytosine·cytosine$^+$ (C·C$^+$) base pairs in four-stranded intercalated cytosine-rich DNA molecules. Stacking is confined to exocyclic keto and amino groups and stacking is not observed between the aromatic heterocycles of the bases. The top C·C$^+$ base pair from one parallel duplex is drawn with solid bonds and hydrogen bonding interactions between the cytosine bases are shown with solid lines. The lower C·C$^+$ base pair from the second intercalated duplex is depicted with open bonds, and hydrogen bonding interactions are drawn with broken lines. Nitrogens are highlighted by stippling. (*B*) Schematic view of four-stranded intercalated d(CCCT) (3) and d(CCCAAT) (5) illustrating the overall architecture of the intercalation motif and the nucleotide numbering scheme. Covalent bonds are drawn with solid lines. Base pairing interactions are illustrated with tapered bonds. The intercalated segment is highlighted by stippled tapered bonds. In the d(CCCAAT) structure, a crystallographic dyad axis (solid oval) exists in the center of the molecule. Symmetry related nucleotides are marked with asterisks.

be around 2 kcal·mol^{-1} (19). Although C—H···O hydrogen bonds were previously noticed between bases (e.g., refs. 20 and 21) and between bases and backbones (e.g., ref. 10) in the crystal structures of oligonucleotides, their systematic formation between the deoxyriboses of two adjacent oligonucleotide backbones described here constitutes the first example of a tertiary nucleic acid folding motif that is extensively stabilized by this type of interaction.

METHODS

The coordinates for the crystal structures of intercalated cytosine-rich nucleic acid fragments determined thus far are deposited in the Nucleic Acid Database (22), and are accessible via NDB ID codes UDD023 for d(CCCT), UDD024 for d(C$_4$), UDF027 for d(TAACCC), and UDF043 for d(CCCAAT). Since the conformations of the intercalated cytosine segments in the crystal structures are sufficiently similar with respect to the observations described here, only two of them were selected for compiling the data given in Tables 1 and 2. These are the high resolution structure of d(CCCT) and, in addition, the d(CCCAAT) structure, solved at 1.85 Å resolution. The former was selected because of its near atomic resolution (1.4 Å) quality, yielding highly accurate geometrical data, the latter because of the presence of additional close contacts between cytidine deoxyribose sugars and adenosine bases. The stacking pattern of adjacent C·C$^+$ base pairs is shown in Fig. 1*A*. The four-stranded structures formed by d(CCCT) and d(CCCAAT) are depicted schematically in Fig. 1*B*, illustrating the overall architecture of the intercalation motif and the nucleotide numbering scheme. The O4′ oxygens and the C1′ and C4′ carbons of the sugar moieties were assumed to be ideally sp^3 hybridized. The positions of H1′ and H4′ hydrogens were calculated assuming C—H bond lengths of 1 Å. In the skeletal

drawings, vectors describing the O4′ lone electron pairs were assigned a hypothetical length of 1.4 Å (10). The lone electron pair pointing to the same side of the furanose ring as the glycosidic bond is termed β lone pair, the other α lone pair (10). Similarly, to analyze the sugar-base interactions in the two structures, the hydrogen positions of ring carbons were calculated on the basis of ideal sp^2 hybridizations for the carbon atoms and C—H bond lengths of 1 Å.

RESULTS AND DISCUSSION

Stacking of Exocyclic Base Atoms from Adjacent Base Pairs. In four-stranded intercalated molecules, neighboring C·C$^+$ base pairs from intercalated duplexes are arranged in a way that virtually no overlap exists between their six-membered aromatic ring systems (Fig. 1*A*). Instead, pairs of exocyclic keto groups and pairs of exocyclic amino groups overlap in an antiparallel fashion with occasional direct interactions of the amino group hydrogen atoms with the heterocycles. While an interaction of the exocyclic amino group with the base ring system has a stabilizing effect (1), overlap between a keto oxygen and the aromatic ring is energetically unfavorable (23). Dipole–dipole interactions between keto groups aligned in a parallel fashion were earlier observed in A-DNA (ref. 24 and references cited therein) and in a DNA dimer duplex with chemical modifications featuring stacked hemiprotonated C·C$^+$ base pairs (25). The latter duplex exhibits only partial stacking between base rings but complete overlap between exocyclic functional groups and ring systems with a separation of 3.44 Å between adjacent base pairs. In the intercalation motif formed by four strands of d(CCCT), the vertical separation between base pairs is approximately 3.15 Å (3). In both structures, destabilizing interactions between the

Table 1. Distance data in angstroms for the O4' α lone pair (α lp)···H1'–C1' and O4'(α lp)···H4'–C4' hydrogen bonds between deoxyriboses from pairs of antiparallel strands

Parameter	α lp···α lp	O4'···O4'	O4'$_b$···C1'$_a$	O4'$_b$···H1'$_a$	O4'$_a$···C1$_b$	O4'$_a$···H1$_b$	O4'$_a$···C4$_b$	O4'$_a$···H4$_b$
		a-strand C1–C2–C3–T4 and b-strand C13–C14–C15–T16 in the d(CCCT) structure						
C1·T16	1.48	3.16	3.19	2.45	—	—	3.46	2.85
C2·C15	1.49	3.27	3.37	2.64	3.34	2.57	3.37	2.65
C3·C14	1.48	3.16	3.24	2.50	3.48	2.89	3.42	2.75
T4·C13	1.44	3.15	3.36	2.68	3.20	2.45	—	—
		b-strand C5–C6–C7–T8 and a-strand C9–C10–C11–T12 in the d(CCCT) structure						
C6·C11	1.12	2.97	3.27	2.70	3.31	2.74	3.25	2.59
C7·C10	1.26	3.05	3.23	2.57	3.36	2.75	3.45	2.92
		a-strand C1–C2–C3–A4 and b-strand C11*–C12*–C13*–A14* in the d(CCCAAT) structure						
C2·C13*	1.49	3.27	3.27	2.55	3.45	2.75	3.31	2.55
C3·C12*	1.09	2.95	3.21	2.57	3.45	2.97	3.27	2.66
A4·C11*	1.20	2.71	2.94	2.46	3.29	2.86	3.31	2.96
Average	1.33	3.08	3.23	2.57	3.36	2.75	3.36	2.74
σ	0.16	0.17	0.12	0.08	0.13	0.21	0.16	0.28
		corresponding average values in the d(C4) structure						
		3.26	3.33	2.54	3.38	2.58	3.48	2.79

Residues with B-DNA type sugar puckers are underlined and those with A-DNA type sugar puckers are in italics. Respective average values for interatomic distances from the 2.3-Å structure of d(C4) (2) were included for comparison.

positively charged ring systems appear to be avoided, with molecular ion–dipole (26) and dipole–dipole interactions (1) as the main contributors to stability.

C—H···O4' Hydrogen Bonds Between Closely Spaced Deoxyriboses. An unusual structural feature of the intercalation motif is the close proximity of sugar-phosphate backbone pairs from intercalated parallel-stranded duplexes. The two strands in close proximity are oriented in an antiparallel fashion, with inter-strand phosphorus–phosphorus separations approximately equal to those between intra-strand phosphorus atoms (Fig. 2A). This arrangement coincides with juxtaposed deoxyribose O4' α lone electron pairs of adjacent sugars from the two strands (Fig. 2). Distances between O4' atoms and between end points of lone pairs are given in Table 1. Projections of the antiparallel strand pair roughly along and perpendicular to base pairs are shown in Fig. 2 A and B, respectively. At first glance, the closely spaced lone electron pairs appear to be in essence a destabilizing feature in the intercalation motif. However, closer examination of the relative arrangements of adjacent sugar moieties from neighboring antiparallel strands reveals that all O4' α lone electron pairs are engaged in C—H···O hydrogen bonds. Thus, the α lone pairs of one strand (termed *b* in Table 1) are directed toward the C1'–H1' bonds

Table 2. Angle data in degrees for the O4'(α lp)···H1'–C1' and O4'(α lp)···H4'–C4' hydrogen bonds between deoxyriboses from pairs of antiparallel strands

Parameter	O4$_b$–H1'$_a$–C1'$_a$	O4$_a$–H1$_b$–C1$_b$	O4$_a$–H4$_b$–C4$_b$
a-strand C1–C2–C3–T4 and b-strand C13–C14–C15–T16 in the d(CCCT) structure			
C1·T16	131	—	119
C2·C15	131	134	128
C3·C14	131	125	119
T4·C13	125	131	—
b-strand C5–C6–C7–T8 and a-strand C9–C10–C11–T12 in the d(CCCT) structure			
C6·C11	117	117	123
C7·C10	124	120	114
a-strand C1–C2–C3–A4 and b-strand C11*–C12*–C13*–A14* in the d(CCCAAT) structure			
C2·C13*	129	127	133
C3·C12*	121	110	120
A4·C11*	109	107	101
Average	124	121	120
σ	7	10	10

Pucker modes denoted as in Table 1.

of sugars from the opposite strand (termed *a* in Table 1). In turn, the O4' α lone pairs of strand *a* are positioned between the C1'–H1' and C4'–H4' bonds of deoxyriboses from strand *b*, giving rise to a system of bifurcated C—H···O4' bonds along the interface of the two strands. Geometrical details for the C—H···O4' hydrogen bonds are given in Tables 1 and 2, and a drawing of the antiparallel backbones with the three hydrogen bonding interactions per deoxyribose pair is depicted in Fig. 3. The corresponding interatomic distance data from the 2.3-Å resolution structure of d(C4) (2) are included in Table 1, for comparison. There appears to be a subtle correlation between the sugar pucker and the interaction mode of the O4' α lone pairs. Thus, the *a* strands with their O4' α lone pairs engaged in one C—H···O4' hydrogen bond per O4' adopt mostly C2'-*endo* puckers, which is the one observed in regular B-DNA, whereas strands *b* with their O4' α lone pairs shared between the C1'–H1' and C4'–H4' bonds adopt mostly A-DNA type C3'-*endo* puckers. However, this relation appears to strictly hold only for nucleotides in the central and thus largely unperturbed core of the intercalation motif with terminal nucleotides adopting a range of puckers, independent of whether they are located in strand *a* or *b*. Moreover, the d(C4) structure solved by Chen and colleagues (2) seems to allow for more plasticity with regard to the interaction mode of O4' α lone pairs, and thus in some cases C—H···O bonds shared between C1'–H1' and C4'–H4' are actually found to originate from O4' α lone pairs on both antiparallel strands in the narrow grooves.

Intra-Cytidine C6—H6···O4' Hydrogen Bonds and Sugar-Base Stacking Interactions. Two further stabilizing interactions occur at certain base pair steps in the crystal structures of d(CCCT) and d(CCCAAT). These are intra-nucleoside C—H···O hydrogen bonds between the β lone pair of deoxyribose O4' and the C6–H6 bond in pyrimidines, and n-π* conjugations between the O4' α lone pair and a base double bond. Close contacts between the β lone pair of O4' and the pyrimidine H6 hydrogen exist when the conformation around the glycosidic-bond is nearly eclipsed with O4'–C1'–N1–C2 torsion angles around 0° (10). In d(CCCAAT), an intra-nucleoside C—H···O4' hydrogen bond occurs in residue C1. In d(CCCT), a similar hydrogen bond exists for nucleotide T8, which loops away from the C·C+ base pair stack and interacts with a symmetry-related thymidine from an adjacent duplex. These interactions are depicted in Fig. 4A and B, respectively, and geometrical details are given in Table 3. The α lone pairs of O4' atoms that are engaged in intra-nucleoside hydrogen bonds are approximately normal to the base planes of the adjacent nucleotides A14* and T8* in the d(CCCAAT) and

Chemistry: Berger *et al.*

Proc. Natl. Acad. Sci. USA 93 (1996)   12119
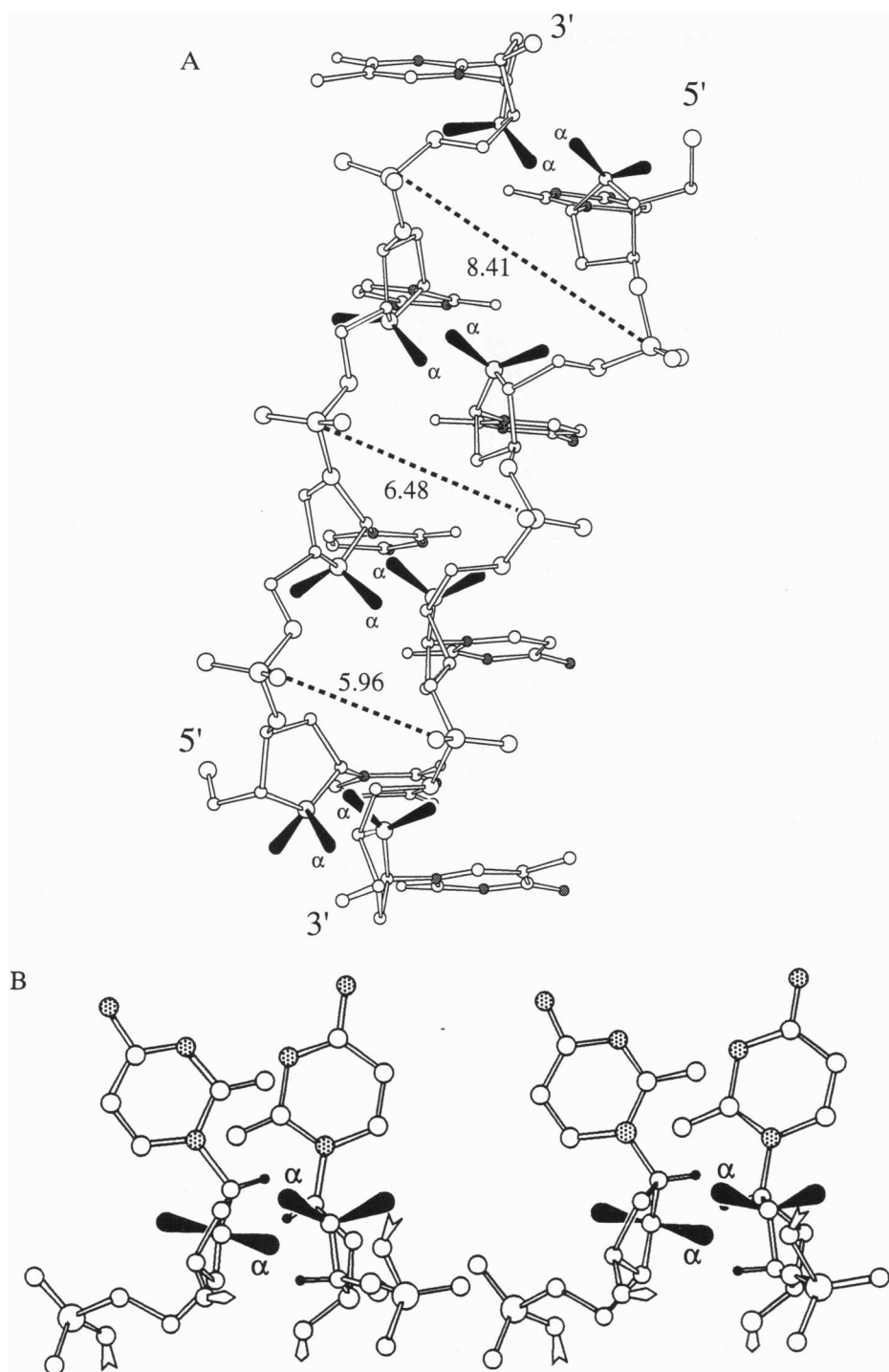
FIG. 2. Juxtaposition of O4′ lone electron pairs. (*A*) Two antiparallel strands in the four-stranded intercalated molecule formed by d(CCCT) (3) viewed from the side, facing a narrow groove. Inter-strand phosphorus–phosphorus distances are illustrated. The O4′ lone electron pairs are filled, α lone pairs are labeled, and nitrogen atoms are highlighted by stippling. The α lone pairs from O4′ oxygen atoms facing each other systematically line up in a parallel fashion throughout the molecule. Strand polarity is indicated by 3′ and 5′ labels. (*B*) Juxtaposition of O4′ lone electron pairs from adjacent antiparallel backbones in a stereoview roughly perpendicular to the helical axis of the four-stranded intercalated molecule in a stereoview depicting two adjacent cytosine residues. The positions of cytosine H1′ and H4′ hydrogen atoms were calculated as described in the text. The α lone pair from the cytosine residue on the right points toward H1′ from its neighbor. The α lone pair from the cytosine residue on the left, however, can interact both with neighboring H1′ and H4′ hydrogen atoms. Strand continuity is indicated by arrows. Hydrogen atoms are depicted as solid spheres.

d(CCCT) structures, respectively (Fig. 4). However, the lone pairs are not directed into the ring system of the bases, but are pointing in the direction of adenine C8 [d(CCCAAT), Fig. 4*A*] and thymine N3 [d(CCCT), Fig. 4*B*]. The observed orientation of the α lone pair of residue C1 relative to the base plane of residue A14* and its C8=N7 double bond (Table 3) in d(CCCAAT) are consistent with an n-π* conjugation (27). Thus, the O4′–C8–N7 angle of 110° would allow optimal overlap between the non-bonded α lone pair of O4′ and the antibonding π* orbital of the C8=N7 double bond. This interpretation is further supported by the fact that the adenine base plane and the plane defined by the N7, C8, and O4′ atoms form a nearly right angle. In the similar interaction between symmetry-related T8 and T8* residues in the d(CCCT) structure, the O4′ α lone pair of the former is positioned approx-

imately normal to the base plane of the latter. This is consistent with the existence of partial N3=C2 and N3=C4 double bonds, and the positioning of the O4′ α lone pair between the π* orbitals associated with them (Fig. 4*B*, Table 3). It is noteworthy that the interactions observed in the base pair steps of the two C-rich structures are very similar to the n-π* conjugation between the O4′ α lone pair of cytidine residues and a postulated partial C2=N2+ double bond in guanidine residues of left-handed Z-DNA (10).

Similar interactions have been seen in RNA macromolecules. Close examination of the earlier noted base-phosphate stacking interactions in the T and anticodon loops of tRNA[Phe] (28) reveals lone pairs of nonbridging phosphate oxygens, which are also directed toward double bonds in bases. For residue U33 in tRNA[Phe], forming the U-turn (28) in the
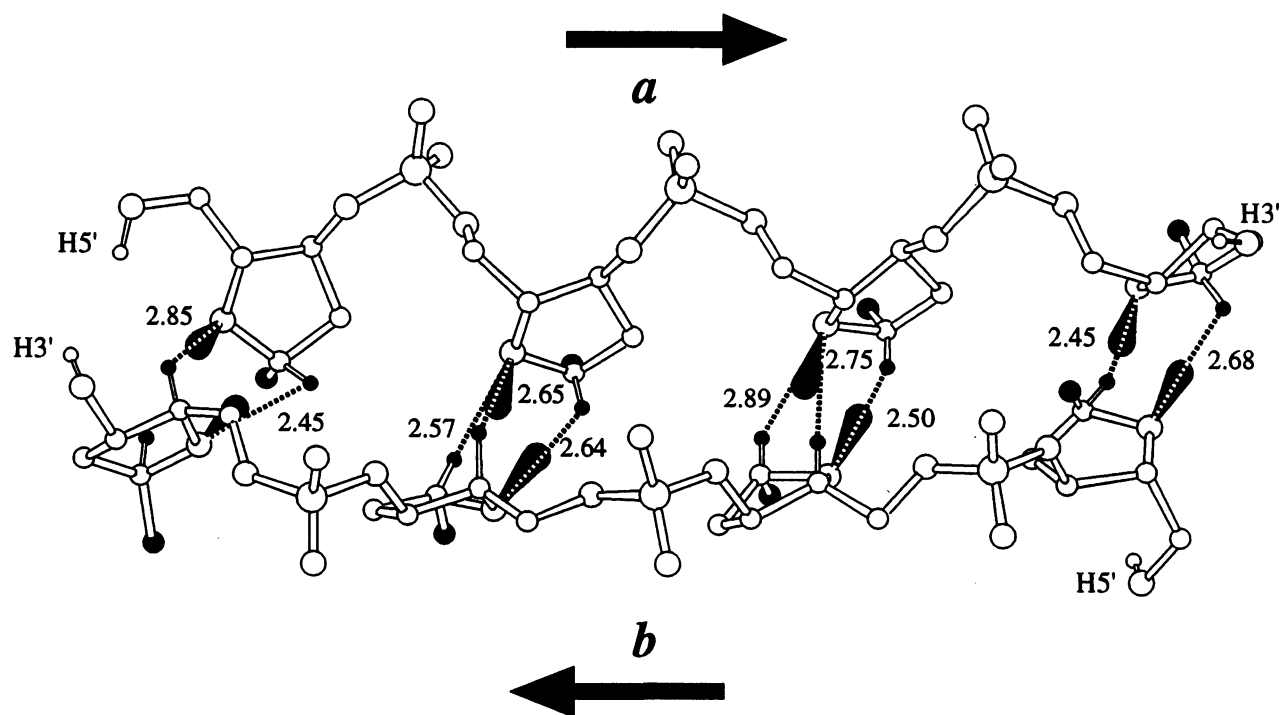
FIG. 3. C—H···O hydrogen bonding network in four-stranded intercalated DNA. Overall view of the C—H···O hydrogen bonding network between O4′ and C1′–H1′ and C4′–H4′ from deoxyriboses of adjacent antiparallel backbones in four-stranded intercalated d(CCCT). Strand polarity is indicated by arrows. O4′ β lone electron pairs are omitted, and only N1 nitrogens (stippled) of the cytosine bases are shown. C—H···O hydrogen bonding interactions are drawn with broken lines. Distances between O4′ oxygens and H1′or H4′ hydrogen atoms are given.
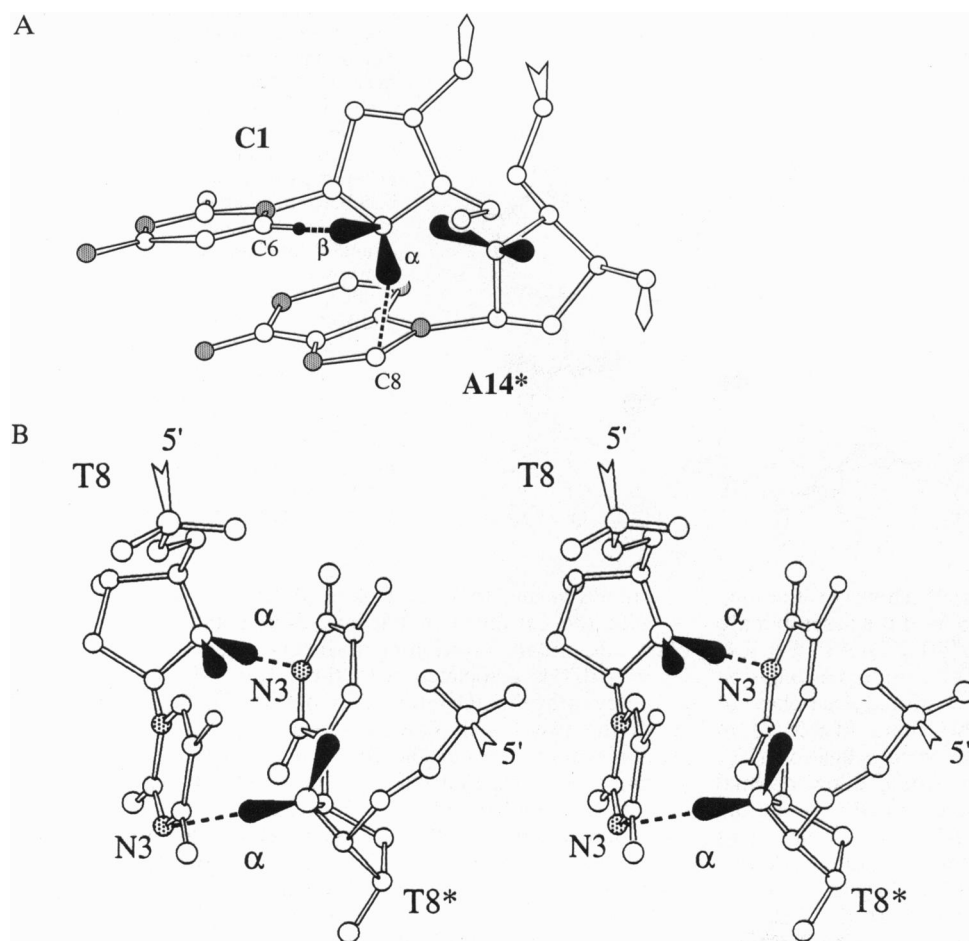
FIG. 4. (*A*) Detailed view of the intra-cytidine O4′ (β lone pair)··· H6–C6 hydrogen bond and the n-π* interaction between the deoxyribose O4′ α lone pair of residue C1 and the C8=N7 double bond from the stacked adenine base of residue A14* in the d(CCCAAT) structure. (*B*) Similar O4′ (β lone pair)···H6–C6 hydrogen bonding and n-π* interactions in symmetry-related terminal thymidines T8 and T8* in the d(C-CCT) structure (stereoview). The O4′ lone electron pairs are filled, H6 hydrogen atoms are depicted as solid spheres, nitrogen atoms are highlighted by stippling, and C—H···O and n-π* interactions are drawn with broken lines.

Table 3. Distances in angstroms and angles in degrees for the O4'(α lp)··base n-π* conjugations and the intra-nucleoside O4'(β lp)···H6–C6 hydrogen bonds for nucleotide pairs T8 and T8* and C1 and A14 and in the d(CCCT) and d(CCCAAT) structures, respectively

Parameter	O4'···T(A)◇	α lp··T(A)◇	O4'···N3	α lp··N3	O4'–N3–C2(4)	O4'–α lp–N3
			O4'(α lp)··base n-π* conjugation			
T8/T8*	2.97	1.65	3.13	1.73	89(75)	177
C1/A14*	2.90	1.51	3.03	1.73	110	150
Parameter	O4'···C6	O4'···H6	O4'–H6–C6	β lp–H6–C6	O4'–β lp–H6	O4'–C1'–N1–C6
			O4'(β lp)···H6–C6 hydrogen bond			
T8	2.74	2.48	94	105	120	41
C1	2.53	2.12	102	124	144	29

T◇ and A◇ are the best planes through the bases of residues T8* and A14*, respectively. Symmetry-related residues are marked with asterisks.

anticodon loop, the n-π* conjugation occurs between its C5=C6 double bond and an oxygen lone pair (O2P of residue 35; O2P···C5 = 3.06 Å; O2P–C5–C6 = 101°). For residue Ψ55, the interaction takes place between its C4=O4 double bond and an oxygen lone pair (O1P of residue 57; O1P···C4 = 3.06 Å; O1P–C4–O4 = 106°). Similar phosphate–uracil base interactions are observed in the U-turn of the hammerhead ribozyme adjacent to the cleavage site (29, 30).

CONCLUSIONS

One of the most surprising features of the intercalation motif adopted by cytosine-rich DNA is the close proximity of pairs of sugar-phosphate backbones, creating inter-strand phosphorus–phosphorus distances, which are typically shorter than those between adjacent intra-strand phosphorus atoms in B-DNA. The Coulomb repulsion resulting from such closely spaced phosphate groups as well as the lack of overlap between the ring systems of stacked cytosines are in apparent contradiction to the ready adoption of the four-stranded conformation by C-rich DNA oligonucleotides. However, our analysis has revealed the existence of a systematic network of C—H···O hydrogen bonds involving the O4', C1', and C4' atoms between the deoxyriboses of the two closely spaced backbones in four-stranded intercalated DNA. These interactions may contribute significantly to the stability of this unusual nucleic acid structure because, apart from a resulting disruption of the C—H···O hydrogen bonds, there is no obvious reason why the two intercalated parallel-stranded duplexes could not be rotated relative to one another around their helical axis to yield increased and thus energetically more favorable inter-strand phosphorus–phosphorus distances in the narrow grooves. While pairing of strands in the familiar right- and left-handed DNA duplex families takes place via base–base interactions, the antiparallel pairing of strands in the intercalation motif occurs through hydrogen bonding interactions between the backbones, somewhat reminiscent of the alignment of peptide strands in antiparallel β-sheets. Other stabilizing factors in addition to these C-H···O hydrogen bonds are the previously noted dipole–dipole (1) and ion–dipole interactions between stacked C·C⁺ base pairs, stereoelectronic effects involving the O4' lone electron pairs, such as the ones found at C-A junctions in the d(CCCAAT) structure, and a zipper-like hydration in one of the wide grooves of the molecule, bridging phosphate groups to hemiprotonated base pairs (3, 5, 6). The latter interaction may effectively moderate the repulsions between phosphates of strands paired via C—H···O hydrogen bonds. Our observation lends further support to C—H···O hydrogen bonding interactions being a recurring stabilization motif in DNA and RNA, on the level of both secondary and tertiary structure. We anticipate that the elucidation of larger, more elaborately folded nucleic acid structures will yield further insight into the contribution of C—H···O hydrogen bonds to nucleic acid conformation.

1. Gehring, K., Leroy, J.-L. & Guéron, M. (1993) *Nature (London)* 363, 561–565.
2. Chen, L., Cai, L., Zhang, X. & Rich, A. (1994) *Biochemistry* 33, 13540–13546.
3. Kang, C. H., Berger, I., Lockshin, C., Ratliff, R., Moyzis, R. & Rich, A. (1994) *Proc. Natl. Acad. Sci. USA* 91, 11636–11640.
4. Leroy, J.-L. & Guéron, M. (1995) *Structure (London)* 3, 101–120.
5. Berger, I., Kang, C. H., Fredian, A., Ratliff, R., Moyzis, R. & Rich, A. (1995) *Nat. Struct. Biol.* 2, 416–425.
6. Kang, C. H., Berger, I., Lockshin, C., Ratliff, R., Moyzis, R. & Rich, A. (1995) *Proc. Natl. Acad. Sci. USA* 92, 3874–3878.
7. Kang, C. H., Zhang, X., Ratliff, R., Moyzis, R. & Rich, A. (1992) *Nature (London)* 356, 126–131.
8. Laughlan, G., Murchie, A. I. H., Norman, D. G., Moore, M. H., Moody, P. C. E., Lilley, D. M. J. & Luisi, B. (1994) *Science* 265, 520–524.
9. Patel, D. J. (1993) *Nature (London)* 363, 499–500.
10. Egli, M. & Gessner, R. V. (1995) *Proc. Natl. Acad. Sci. USA* 92, 180–184.
11. Taylor, R. & Kennard, O. (1982) *J. Am. Chem. Soc.* 104, 5063–5070.
12. Jeffrey, G. A. & Saenger, W. (1991) *Hydrogen Bonding in Biological Structures* (Springer, New York).
13. Desiraju, G. R. (1995) *Angew. Chem. Int. Ed. Engl.* 34, 2311–2327.
14. Jeffrey, G. A., Maluszynska, H. & Mitra, J. (1985) *Int. J. Biol. Macromol.* 7, 336–348.
15. Leonard, G. A., McAuley-Hecht, K., Brown, T. & Hunter, W. N. (1995) *Acta Crystallogr. D* 51, 136–139.
16. Steiner, T. (1995) *Acta Crystallogr. D* 51, 93–97.
17. Auffinger, P., Louise-May, S. & Westhof, E. (1996) *J. Am. Chem. Soc.* 118, 1181–1189.
18. Derewenda, Z. S., Lee, L. & Derewenda, U. (1995) *J. Mol. Biol.* 252, 248–262.
19. Seiler, P., Weisman, G. R., Glendening, E. D., Weinhold, F., Johnson, V. B. & Dunitz, J. D. (1987) *Angew. Chem. Int. Ed. Engl.* 26, 1175–1177.
20. Egli, M., Gessner, R. V., Williams, L. D., Quigley, G. J., van der Marel, G. A., van Boom, J. H., Rich, A. & Frederick, C. A. (1990) *Proc. Natl. Acad. Sci. USA* 87, 3235–3239.
21. Portmann, S., Grimm, S., Workman, C., Usman, N. & Egli, M. (1996) *Chem. Biol.* 3, 173–184.
22. Berman, H. M., Olson, W. K., Beveridge, D. L., Westbrook, J., Gelbin, A., Demeny, T., Hsieh, S.-H., Srinivasan, A. R. & Schneider, B. (1992) *Biophys. J.* 63, 751–759.
23. Hozba, P., Sponer, J. & Polasek, M. (1995) *J. Am. Chem. Soc.* 117, 792–798.
24. Shakked, Z., Rabinovich, D., Kennard, O., Cruse, W. B. T., Salisbury, S. A. & Vismamitra, M. A. (1983) *J. Mol. Biol.* 166, 183–201.
25. Egli, M., Lubini, P., Bolli, M., Dobler, M. & Leumann, C. (1993) *J. Am. Chem. Soc.* 115, 5855–5856.
26. Sponer, J., Leszczynski, J., Vetterl, V. & Hozba, P. (1996) *J. Biomol. Struct. Dyn.* 13, 695–706.
27. Bürgi, H. B., Dunitz, J. D. & Shefter, E. (1973) *J. Am. Chem. Soc.* 95, 5065–5067.
28. Quigley, G. J. & Rich, A. (1976) *Science* 194, 796–806.
29. Pley, H. W., Flaherty, K. M. & McKay, D. B. (1994) *Nature (London)* 372, 68–74.
30. Scott, W. G., Flinch, J. Y. & Klug, A. (1995) *Cell* 81, 991–1002.